Editors' Suggestion

Exciton formation dynamics in (Ga,In)As quantum wells

D. Anders [1], F. Dobener [1], C. Fuchs,[2] K. Volz,[2] S. Chatterjee [1], and M. Stein [1,*]

[1]*Institute of Experimental Physics I and Center for Materials Research (LaMa), Justus-Liebig-University Giessen, Heinrich-Buff-Ring 16, D-35392 Giessen, Germany*

[2]*Structure & Technology Research Laboratory (WZMW), Philipps-University Marburg, Hans-Meerwein-Straße 6, D-35032 Marburg, Germany*

(Received 1 August 2025; revised 24 October 2025; accepted 27 October 2025; published 1 December 2025)

We investigate the ultrafast dynamics of exciton formation in (Ga,In)As quantum wells using optical pump–terahertz probe spectroscopy, complemented by time-resolved photoluminescence. Terahertz spectroscopy directly probes intraexcitonic transitions and thus, in principle, distinguishes between unbound electron-hole plasma and Coulomb-bound exciton populations. At low excitation densities, this separation is effective: the Drude response of the electron-hole plasma remains spectrally distinct from narrow intraexcitonic resonances. However, at higher excitation densities, spectral broadening and overlap obscure this distinction.

Following low-density nonresonant excitation, we initially observe a pure Drude-like plasma response that gradually transitions into an intraexcitonic resonance. In contrast, at higher excitation densities, conventional analysis based on the Drude-Lorentz model suggests questionably high exciton fractions up to 32% immediately after excitation. It remains uncertain whether these fractions represent genuine instantaneous exciton formation or arise from spectral overlap and analytical ambiguity. To resolve this, we introduce a differential probing technique utilizing exciton ionization induced by strong THz fields. By comparing responses obtained at high and low THz field strengths, we isolate the exciton contribution from the pure plasma contributions. This approach reveals intrinsic exciton formation dynamics governed by two characteristic timescales: a fast component in the vicinity of 10 ps and a slower process around 250 ps. Notably, these timescales remain largely independent of excitation density, contrasting sharply with the strong density dependence suggested by conventional methods.

Our results establish a robust method to disentangle exciton and plasma dynamics, providing clearer insight into exciton formation under nonresonant excitation in semiconductor quantum wells.

DOI: 10.1103/jb2l-zrc3

I. INTRODUCTION

The widespread availability of pulsed and ultrafast laser systems has spurred vast research efforts to identify quasiparticle dynamics in condensed matter systems, such as studying charge carriers in semiconductors and their heterostructures [1–3]. Among these, the formation dynamics of excitons, i.e., a quasiparticle many-body state consisting of an electron and a hole stabilized by Coulomb attraction, has often been controversially discussed [4,5]. The prominent spectral features in the vicinity of the band-gap energy associated with excitons dominate the linear optical response in many high-quality semiconductors, ranging from bulk inorganic compound materials or organic semiconductors to quantum structures and novel materials including two-dimensional (2D) materials and layered van der Waals heterostructures. Traditionally, excitons and their dynamics have been investigated primarily by time-resolved photoluminescence (TRPL) spectroscopy [6–12]. However, photoluminescence spectroscopy inherently accesses only bright excitons, i.e., those with a center-of-mass momentum close to zero. This limits its ability to capture the entire exciton population and complicates the interpretation of formation dynamics [5,13]. Consequently, the reported exciton formation times extracted from TRPL spectroscopy on GaAs-based quantum well structures vary by more than one order of magnitude from less than 20 ps [6,7,9–11] to more than 200 ps [4,14]. Later, stringent theoretical analysis has revealed that the sources of emission at the $1s$ exciton energy are not limited to exciton population decay [15]. Subsequently, these theoretical findings have been substantiated experimentally [16,17]. Optical pump–terahertz probe (OPTP) spectroscopy has since been proposed as a more direct and unambiguous method to investigate exciton formation [5,18,19]. THz pulses directly probe intraexcitonic transitions and provide distinct signatures of Coulomb-bound excitons, such as the $1s-2p$ absorption resonance, which are absent in the Drude-like response of unbound electron-hole plasmas. Moreover, terahertz spectroscopy is sensitive to excitons of any center-of-mass momentum, making it a versatile tool for tracking exciton populations [5,19–21]. However, despite these methodological advantages, OPTP spectroscopy has not provided a consistent picture of the exciton formation dynamics in GaAs-based quantum wells after nonresonant excitation. Reported results span a broad

*Contact author: markus.stein@exp1.physik.uni-giessen.de

range: some studies observe relatively slow exciton formation over several-hundred picoseconds [17,22], while others report ultrafast formation, with up to 40% of the exciton population emerging within just a few picoseconds [20,23], and yet others report intermediate timescales [24].

In this work, we introduce a different approach to disentangle Coulomb-bound exciton and unbound electron-hole plasma contributions in time-resolved THz spectroscopy of high-quality (Ga,In)As/GaAs multiple quantum wells (MQWs) after nonresonant excitation. By systematically varying the field strength of the probing THz pulse, we exploit field-induced exciton ionization at high THz fields to selectively switch off the excitonic response and compare these measurements with low-field conditions that preserve the exciton population. This differential probing technique isolates the exciton response from the plasma background, even at high excitation densities, where, in conventional analysis, spectral overlap typically obscures the distinction between excitons and free carriers.

Using this method, we uncover intrinsic exciton formation dynamics governed by two distinct timescales: a fast component of approximately 10 ps and a slower process of about ∼250 ps, both largely independent of excitation density. Our results resolve longstanding ambiguities related to apparently instantaneous exciton formation reported in earlier OPTP studies and establish a robust framework for probing ultrafast exciton formation dynamics in semiconductor quantum structures.

II. EXPERIMENTAL DETAILS

The samples under investigation are (Ga,In)As MQW structures grown by metal organic vapor phase epitaxy on a GaAs substrate. The primary MQW structure (1) consists of 50 periods of 1.35 nm GaAs, 8.65 nm (Ga,In)As, 1.35 nm GaAs, and 8.65 nm Ga(As,P); In and P concentrations are 9.5% and 22%, respectively; details of the sample structure are given elsewhere [25]. The second sample (2) also consists of 50 periods of different layer widths: 4.6 nm GaAs, 7.6 nm (Ga,In)As, 4.6 nm GaAs, and 19.4 nm Ga(As,P); the In and P concentrations are 5.8% and 5.3%, respectively [22]. All experiments are performed under cryogenic conditions at a lattice temperature of 6 K to minimize broadening and phonon scattering. The OPTP setup utilizes a 5 kHz repetition rate regenerative amplifier that generates 50 fs pulses centered at 800 nm. These pulses are split into two paths using a beam splitter. One part drives an optical parametric amplifier that generates the optical pump at a central wavelength of about 850 nm. After the light has passed a delay line, a grating pulse shaper finely adjusts the pulse to the desired wavelength and spectral width before exciting the sample. The second part of the regenerative-amplifier output is divided by another beam splitter. The largest part of the pulse is directed through a second delay line to a large-aperture GaAs antenna which delivers single-cycle THz pulses. An ellipsoidal mirror focuses the THz pulses onto the sample where they spatially overlap with the optical pump beam. Another ellipsoid relays the transmitted THz pulse onto a 500-μm-thick ZnTe crystal. The THz beam path is continuously purged with dry nitrogen gas to prevent spurious spectral signatures related to absorption by water vapor in the ambient atmosphere. The transient THz electric field is measured via electro-optic sampling using a third optical pulse. This configuration probes the sample's response in the energy range of 0.8 to 12.5 meV (0.2–3.0 THz). We sample 12-ps-long THz time traces and apply a Blackman-Nutall window function with a 2 ps slope before Fourier transforming the data into the frequency domain. By measuring the THz waveform of the unexcited sample, $E(t)$, and its excitation-induced change, $\Delta E(t)$, we calculate the complex dielectric function of the sample [26],

$$\Delta\epsilon(\omega) = \frac{2ic_0\sqrt{\epsilon_r}}{\omega L}\left(\frac{\Delta E(\omega)}{E(\omega)}\right), \tag{1}$$

where c_0 is the speed of light in vacuum and ϵ_r is the dielectric constant of the material.

TRPL measurements are performed using a typical streak camera setup in reflection geometry. Excitation is provided by a Ti:sapphire laser oscillator that emits 100 fs pulses at a repetition rate of 78 MHz and a center wavelength of 850 nm. The excitation light is focused on a 40-μm-diameter spot using a confocal beam path for both excitation and detection. The emitted PL signal is spectrally dispersed by a spectrograph equipped with a 122 lines mm grating, while temporal resolution is provided by a streak camera with an S20 cathode featuring an instrument response <1 ps.

III. RESULTS

We excite the sample nonresonantly, i.e., at energies greater than the 1*s* exciton resonance, to investigate the exciton formation dynamics. All photon densities are kept comparable at around 4×10^{12} cm^{-2}, corresponding to $2 \times I_0$. The linear absorption spectra of the primary and secondary samples are shown in Figs. 1(a) and 1(b), together with the corresponding pulses for nonresonant excitation. The sample's response is probed by ∼1-ps-long THz pulses for different time delays Δt between the optical pump and the THz probe pulse. The delay is scanned from −5 ps, i.e., the probe impinges on the sample before the pump, to 1800 ps after the pump pulse maximum. The absorption and the change of the dielectric function exclusively show a Drude-like response during the first 3 ps. This clearly indicates the presence of a purely uncorrelated electron-hole plasma [cf. Figs. 2(a) and 2(b), top row]. Subsequently, the absorption in the energy range around 7 meV increases within the next few picoseconds. This is accompanied by an increase in the change of the dielectric function below 7 meV. Both are indicative of the incipient formation of an incoherent exciton population. Finally, a characteristic peak at 7.4 meV develops in the absorption spectrum on a timescale of several-hundred picoseconds. This resonance is directly related to the typical zero crossing of a Lorentzian response in the real part of the dielectric function change [Figs. 2(a) and 2(b), bottom row]. Both are unambiguous signatures for the presence of a 1*s* exciton population. The 1*s* exciton population coexists with the remanent electron-hole plasma that has not yet been converted into an exciton population, as shown by the superimposed Drude response. We quantify the exciton formation dynamics by a phenomenological Drude-Lorentz model reproducing the experimental data. Fitting the change of the real part of the dielectric function

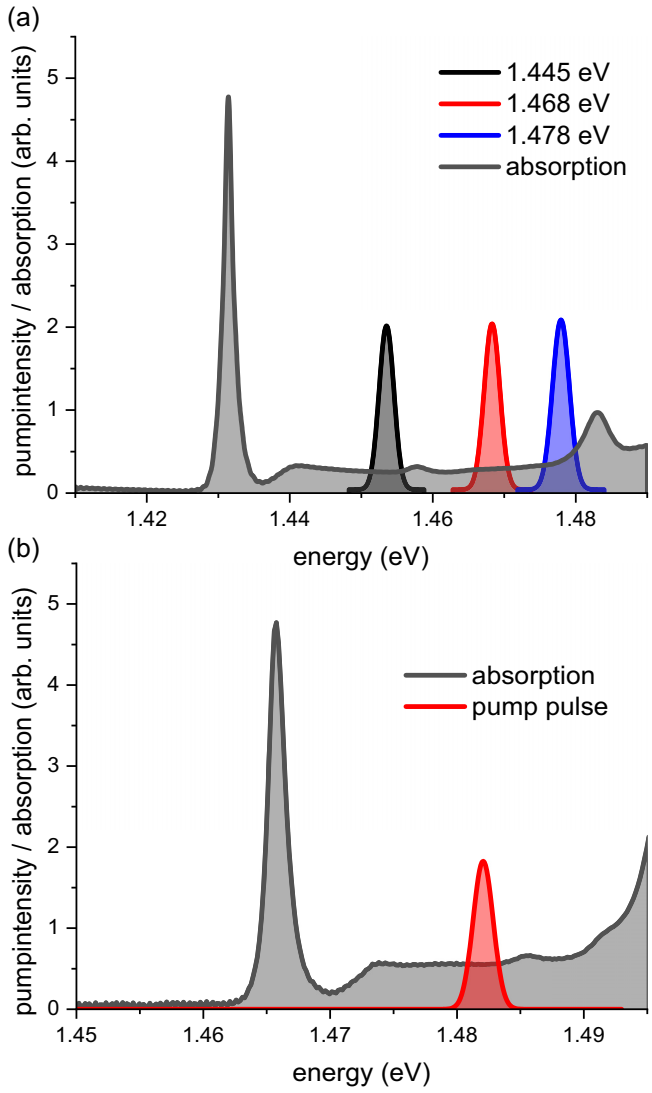

FIG. 1. (a) Linear absorption spectrum of sample 1, overlaid with the excitation pulses used for different excess energies. (b) Absorption spectrum of sample 2 along with the corresponding excitation pulse.

$\Delta\epsilon(\omega)$ and the change in absorption $\Delta\alpha(\omega)$ simultaneously yields robust results. This model accounts for the two components and describes the excitation-induced changes of the complex dielectric function by the following equation [27,28]:

$$\Delta\epsilon(\omega) = \frac{e^2}{L\epsilon_0\mu}\left(\underbrace{\frac{f_{1s-2p}n_x}{\omega_{\text{res}}^2 - \omega^2 - i\omega\Delta_{\text{hom}}}}_{\text{I: Intraexcitonic absorption}} - \underbrace{\frac{n_{fc}}{\omega^2 + i\omega\Gamma}}_{\text{II: Drude response}}\right). \tag{2}$$

The first part (I) corresponds to the Lorentzian lineshape of the intraexcitonic $1s-2p$ transition. Its oscillator strength is f_{1s-2p}, the resonance frequency ω_{res}, the exciton sheet density n_x, and the homogeneous linewidth Δ_{hom}. The second part (II) describes the Drude response characteristic for unbound carriers. It includes both the carrier sheet density n_{fc} and the carrier scattering rate Γ. Parameters that remain constant across all fits include the thickness of the sample L, the effective mass μ, the electron charge e, the vacuum permeability ϵ_0, and the intraexcitonic oscillator strength f_{1s-2p}. Thus, the Drude-Lorentz model provides direct access to the density of Coulomb-bound $1s$ excitons n_{x} as well as the density of free charge carriers n_{fc}, i.e., the electron-hole plasma, in the sample. Shortly after optical excitation, the exciton density rises rapidly from a pure electron-hole plasma, reaching approximately 30% to 50% of its maximum value within 40 ps. Around 600 ps after excitation, the exciton density peaks before gradually decreasing on a nanosecond timescale due to radiative and nonradiative recombination processes. A tri-exponential fit to the exciton density extracted at each time step using the Drude-Lorentz model function quantitatively describes the exciton formation and decay dynamics. The decay is well described by a single exponential term. However, the rise of exciton density requires two distinct exponential components to achieve an accurate representation, indicating the presence of multiple formation timescales. The extracted exciton densities are shown in Fig. 2(c) along with the tri-exponential fit. For comparison, a bi-exponential fit is also included, highlighting the necessity of incorporating both fast and slow rise components to fully capture the formation dynamics. The time constants reveal the following three characteristic regimes:

(i) a rapid exciton formation process with a time constant in the vicinity of 20 ps,

(ii) a significantly slower formation process with a time constant around 300 ps, and

(iii) a subsequent population decay with a time constant of about 1.5 ns.

A comparison of the results for the three different optical excitation energies of 1.445 eV (black), 1.468 eV (red), and 1.478 eV (blue) reveals a strikingly similar response. This suggests that the observed exciton formation dynamics are characteristic of nonresonant excitation conditions that are not too high in energy above the exciton resonance. The corresponding excess energies relative to the $1s$ exciton state are 14, 37, and 47 meV, respectively. Notably, the excess energy of 37 meV (1.468 eV excitation energy) is close to the optical phonon energy in (Ga,In)As of approximately 36 meV. Several theoretical works have proposed that exciton formation could be particularly efficient when the carrier excess energy matches the longitudinal optical (LO) phonon energy, as LO-phonon emission may provide an efficient channel for energy relaxation and exciton binding [29–32]. However, in our experiments, we do not find any clear evidence of enhanced exciton formation efficiency when the excitation excess energy coincides with the optical phonon energy. This observation is consistent with other experimental reports that found no correlation between exciton formation dynamics and an excess energy resonant with the LO-phonon energy [7].

The timescales of exciton formation in GaAs-based quantum structures have been extensively debated, with reported values ranging from less than 20 ps [6,7,9–11] to several-hundred picoseconds [4,14]. Our results indicate that both timescales coexist: an initial rapid exciton formation, followed by a slower secondary process. This dual-process behav-

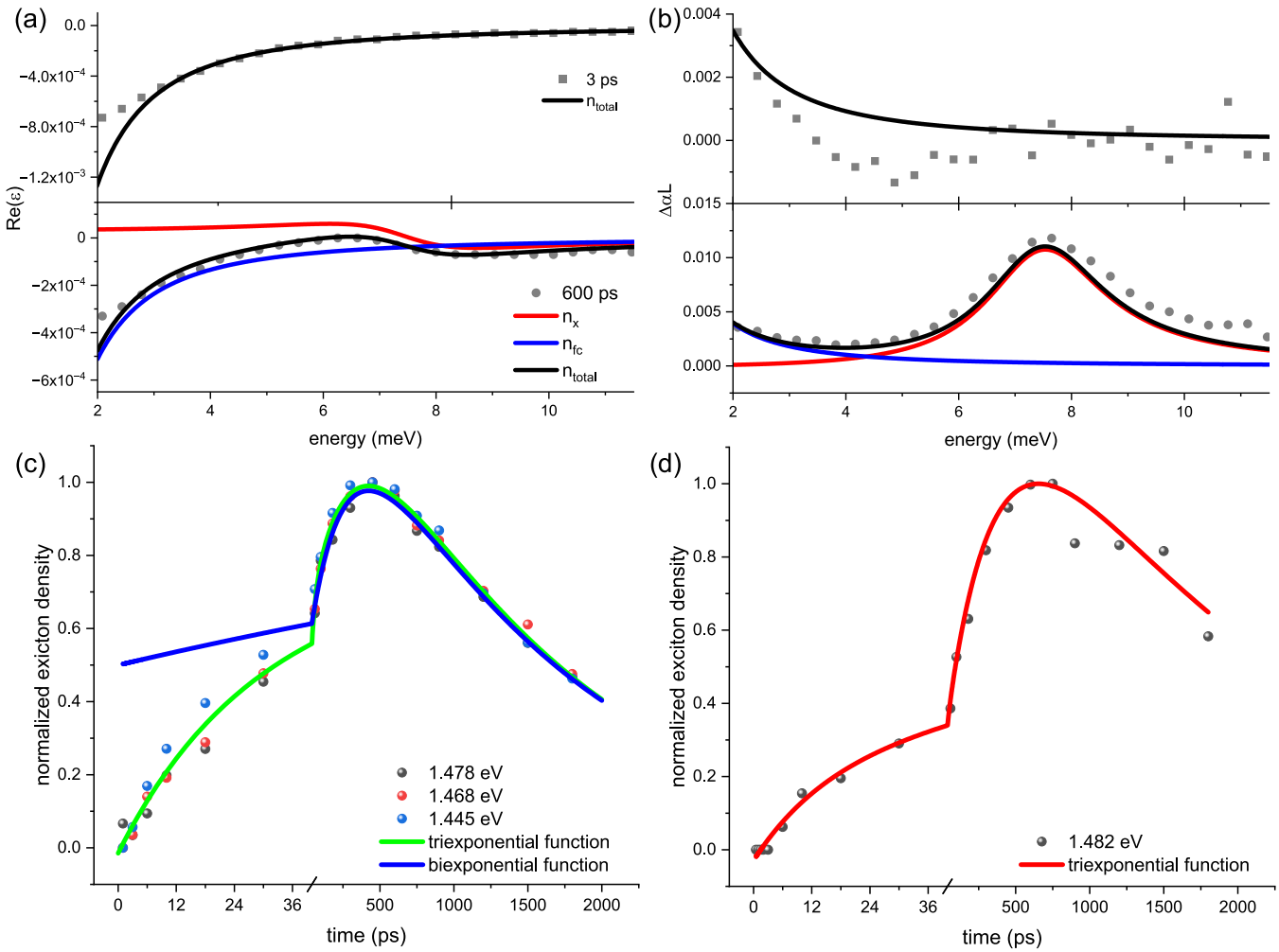

FIG. 2. (a) Pump-induced change of the absorption $\Delta\alpha$L and (b) real part of the dielectric function for delays of 3 ps (top) and 600 ps (bottom). The corresponding fits are shown as colored lines. The different contributions of free and bound electron-hole pairs are indicated for a delay of 600 ps. (c) The normalized exciton densities with bi-exponential and tri-exponential fits for the different excitation energies for the first sample; (d) the normalized exciton density for the control sample.

ior aligns qualitatively with previous observations by Kaindl *et al.* in GaAs quantum wells using OPTP spectroscopy [20,23]. To assess the robustness of this behavior, we repeated the measurements on a second (Ga,In)As MQW sample (sample 2), with different indium content and well width. In Fig. 2(d), we present data from the second sample excited at an energy of 1.482 eV (corresponding to an excess energy of 16 meV) at a comparable photon density. The exciton formation dynamics in this sample are similar to those observed in sample 1, indicating that the dual-component formation process is largely independent of specific structural parameters, provided the exciton binding energy remains similar.

Since TRPL remains a common tool to assess exciton formation dynamics, we compared TRPL and OPTP measurements directly in Fig. 3 [4,13,33–35]. Under identical excitation conditions (1.458 eV, 2.75 × I_0), the PL signal reaches its maximum at the exciton resonance (∼1.428 eV) within the experimental resolution (∼39 ps), consistent with previous reports [16]. In contrast, the THz response reveals no evidence of a significant exciton population immediately after excitation. Instead, the intraexcitonic absorption at 7.4 meV peaks only after several-hundred picoseconds. This discrepancy arises as the PL emitted at an exciton resonance energy does not necessarily require a preexisting population of excitons. As established in prior theoretical and experimental studies [15–17], PL at the exciton resonance can also originate from a pure electron-hole plasma without the formation of Coulomb-bound excitons. In contrast, THz absorption near 7 meV directly probes intraexcitonic transitions and thus provides a more definitive measure of the exciton population. Consequently, PL dynamics mainly reflect recombination of the entire carrier ensemble, while THz spectroscopy captures the actual buildup of Coulomb-bound excitons. As a result, the photoluminescence dynamics exhibit a much stronger correlation with the plasma dynamics of the OPTP spectroscopy than with its exciton formation process. This is illustrated in Fig. 3(c), where the temporal evolution of the electron-hole plasma extracted from the OPTP data is directly compared to the PL from the excitonic resonance. Apart from an initial PL overshoot caused by scattered excitation light, both signals exhibit nearly identical temporal dynamics.

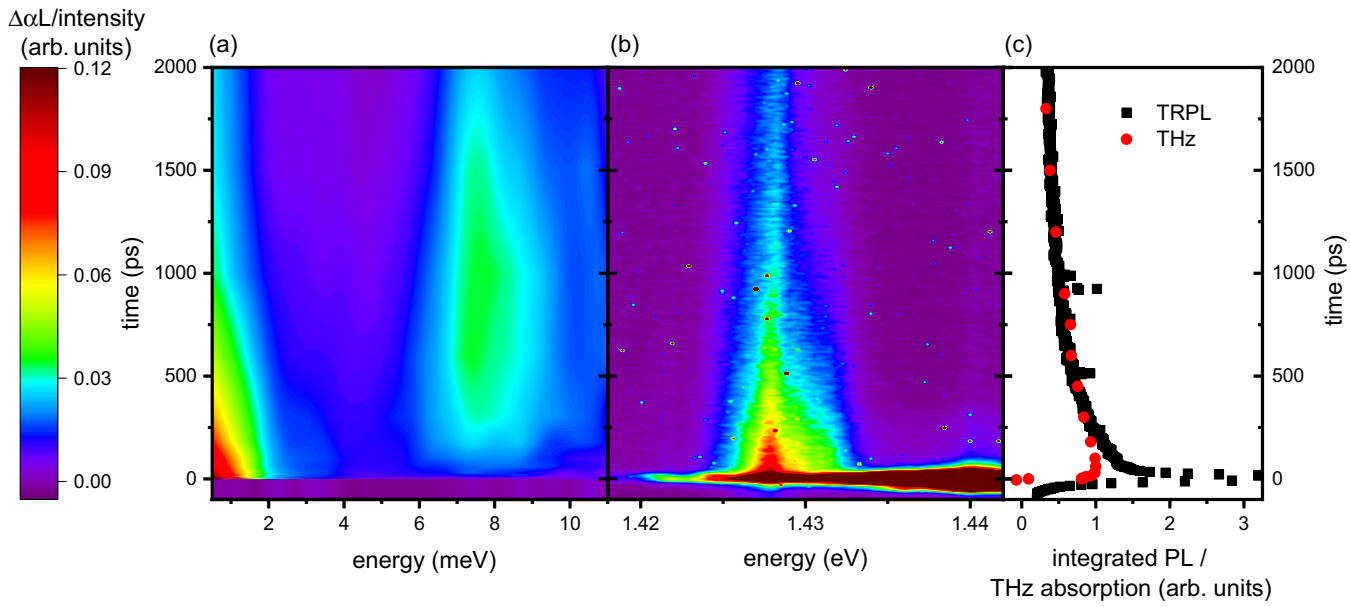

FIG. 3. (a) Optical pump–terahertz probe absorption and (b) time-resolved photoluminescence. An optical pulse with a central energy of 1.458 eV and a density of $2.75 \times I_0$ is applied in both experiments. (c) The integral of the plasma from (a) and the corresponding integrated PL from (b). The THz data were integrated from 0.5 to 2 meV and the PL data were integrated from 1.426 to 1.429 eV.

We further explore exciton formation for systematically varied excitation densities using OPTP spectroscopy since charge-carrier dynamics are highly density dependent [21,36,37]. Figure 4 presents the pump-induced change in absorption, $\Delta\alpha L$, and the real part of the dielectric function for a pump energy of 1.468 eV at three different photon densities. While the overall spectral features of the THz response remain qualitatively similar across excitation densities, increasing the carrier density leads to markedly broader intraexcitonic absorption peaks and flatter dielectric function profiles [cf. Fig. 4(a)]. These trends are consistent with enhanced carrier-carrier scattering in a denser environment [27,38]. The Drude-like plasma response increasingly overlaps with the spectral range of intraexcitonic transitions for the highest excitation density investigated (1.08×10^{13} photons/cm^2). This renders a clear separation of excitonic and plasma contributions challenging—even considering the sensitivity of OPTP spectroscopy. Consequently, the interpretation of the data is less unambiguous than for lower excitation densities. Explicitly, the analysis reveals higher exciton fractions almost instantaneously after excitation, even after carefully restricting the fitting parameters in the Drude-Lorentz model. For our data, we chose a maximum width $\Delta_{\mathrm{hom,max}}$ of 6 meV and a minimum resonance energy $\omega_{\mathrm{res,min}}$ of 4.2 meV. The typical homogeneous line width $\Delta_{\mathrm{hom,max}}$ for low excitation densities is 2.5 meV and a broadening by a factor of about 2.4 is considerable. For the resonance energy, $\omega_{\mathrm{res,min}}$ implies a decrease in exciton binding energy by 53%. We find these barriers to be a sound choice since they still allow the fits to be in good agreement with the data while inhibiting any pathological values. Similarly to our results at higher excitation densities, evidence for an almost instantaneous emergence of a significant exciton population embedded within the broad Drude response has also been reported in the literature using OPTP spectroscopy in GaAs-based quantum structures [20,23]. However, while they report a quasi-instantaneous formation of a 40% exciton population directly after nonresonant excitation, we only observe such a quasi-instantaneous formation for higher excitation densities of $5.3 \times I_0$. For lower excitation densities, our data reveal a finite formation time of tens of picoseconds before reaching comparable exciton fractions. Consequently, at lower excitation densities, it takes approximately 30 ps for the exciton population to build up to levels similar to the "quasi-instantaneous" exciton population observed at higher excitation densities. This abrupt transition from a fast exciton formation to a quasi-instantaneous exciton formation at a specific excitation density prompts several inquiries. First, what physical mechanism emerging above a certain carrier density could enable such an apparently instantaneous exciton formation that is absent at lower densities? Second, does this behavior represent a genuine physical process or is it an artifact arising from the increasingly complex separation of excitonic and electron-hole plasma responses at high excitation densities? To validate the latter, a different method is required to disentangle the contributions of the Drude-like plasma response and the Lorentzian intraexcitonic transition. One way to ensure a pure electron-hole plasma is to ionize the excitons by sufficiently strong THz fields [39–41].

Tuning the pump pulse resonantly to the 1s exciton absorption line allows for the direct generation of a pure exciton population. This bypasses the Drude-like response of an electron-hole plasma, provided that the pump density is sufficiently below the Mott density [37]. In Fig. 5, we monitor the pump-induced change of absorption of sample 2 for various THz field strengths. At low THz probe field strengths, we observe a clean Lorentzian response characteristic of a Coulomb-bound exciton population. As the THz field increases, the spectrum broadens and develops a Drude-like component below 4 meV, indicating the coexistence of unbound carriers. At the highest applied field of 3577 V/cm, the

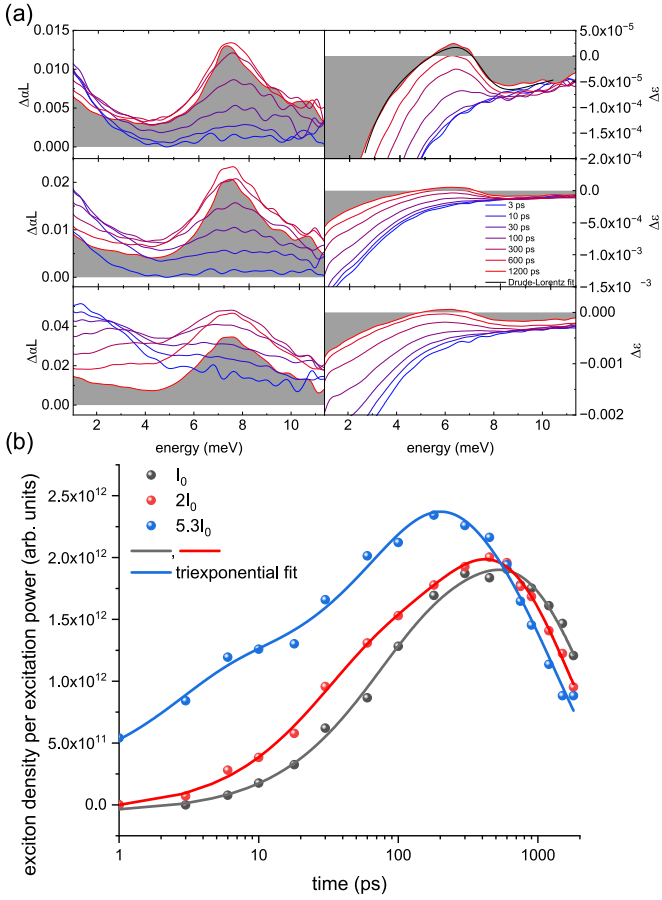

FIG. 4. (a) Experimental THz probe response after optical excitation at 1.468 eV for photon densities of I_0, $2 \times I_0$, and $5.3 \times I_0$. The left column depicts the change in absorption, $\Delta\alpha L$, and the right column shows the change of the real part of the dielectric function, $\Delta\epsilon$. (b) Comparison of the normalized exciton density for three different excitation densities with an excitation energy of 1.468 eV. The colored circles represent the exciton density from the Drude-Lorentz fits, while the solid lines correspond to tri-exponential fits.

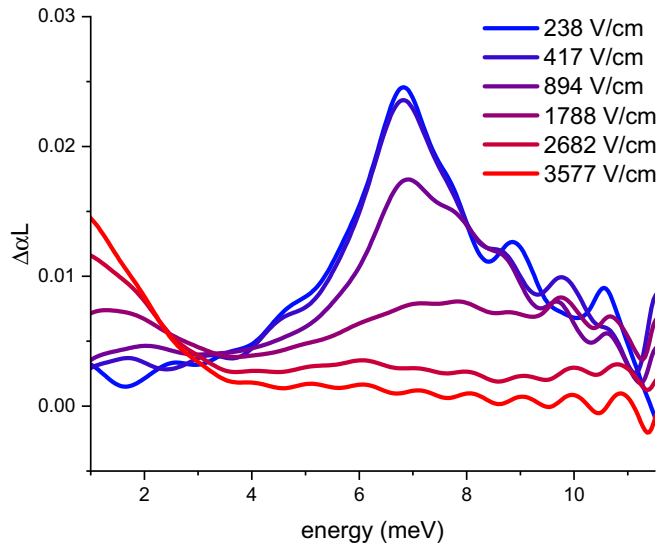

FIG. 5. $\Delta\alpha L$ of sample 2 after resonant excitation for different field strengths of the probing THz pulse.

response is purely Drude-like, signaling complete ionization of the exciton population. These observations demonstrate that by tuning the THz probe field strength, we can effectively switch between a predominantly excitonic system and a pure electron-hole plasma.

Using this approach, we investigate exciton formation dynamics under nonresonant excitation by comparing the sample response under weak and strong THz probe fields. In Fig. 6(a), a weak THz field of ∼238 V/cm yields an initial Drude-like response at 3 ps, which evolves into a Lorentzian profile at later times—indicative of exciton formation out of the electron-hole plasma. In contrast, Fig. 6(b) shows the response under identical excitation conditions, but for a strong THz field of ∼3577 V/cm. Here, although the early-time response is again Drude-like, no Lorentzian feature emerges at later delays because of efficient exciton ionization by the strong THz field. However, a gradual reduction in the Drude response reflects ongoing radiative and nonradiative carrier recombination. To isolate the excitonic contribution, we subtract the strong-field response from the weak-field response. This procedure removes the response of a pure electron-hole plasma from the total response of the sample, which may contain both exciton and plasma contributions. This effectively separates out the exciton dynamics. In the absence of excitons, this subtraction would ideally yield a flat zero line, as the two plasma responses cancel each other. However, in practice, the strong THz field slightly perturbs the carrier distribution, leading to modifications of the carriers' effective mass. This results in a slightly stronger THz absorption especially at lower energies, arising from an enhanced plasma response when probing with strong THz pulses. In contrast, when excitons are present, subtracting the strong-field spectrum removes the Drude-like plasma background and unveils a more distinct intraexcitonic resonance. In addition, a negative differential absorption emerges at low energies. This negative signal occurs because the strong THz field ionizes excitons, thereby increasing the density of unbound carriers which amplifies the plasma response. Subtracting this stronger plasma contribution from the weak-field spectrum results in a net negative differential signal in the corresponding spectral region. This behavior is illustrated across all time delays in Fig. 6(c). Immediately after excitation, the differential absorption signal between 4.1 and 9.3 meV is essentially zero, indicating the absence of a Coulomb-bound exciton population. This directly rules out any instantaneous exciton formation. At lower energies, a weak negative signal is already present at early delays. This is attributed to the strong THz field slightly perturbing the carrier momentum distribution, thereby modifying the slope of the Drude response and leading to small deviations from perfect cancellation in the subtraction. With increasing time delay, a Lorentzian-shaped absorption feature emerges in the 5–9 meV range, which is characteristic of the intraexcitonic $1s - 2p$ transition. Simultaneously, the plasma response below ∼2.5 meV becomes increasingly negative. This trend is expected: the strong THz field ionizes the growing exciton population, thereby increasing the density of unbound carriers and enhancing the Drude-like plasma response. The resulting negative differential signal reflects this excess plasma contribution. To quantitatively assess exciton formation using this method, we integrate the differential THz absorption in the

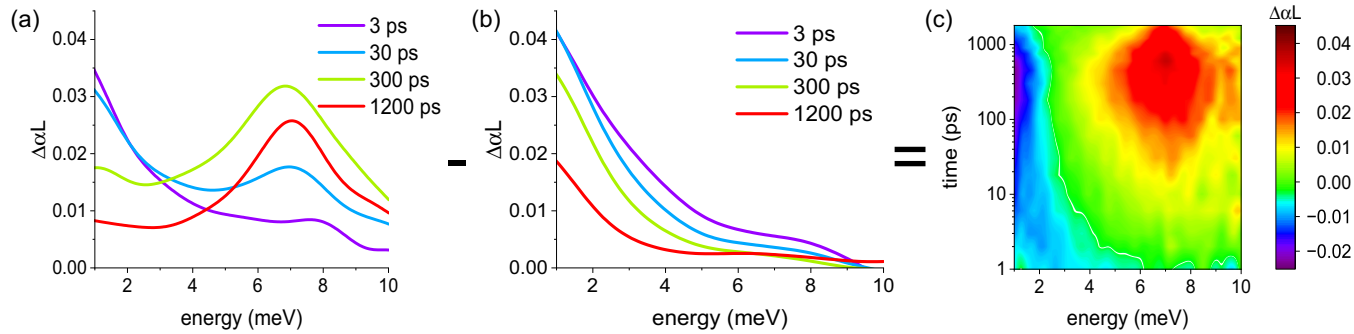

FIG. 6. Pump-induced change of the absorption, $\Delta\alpha L$, for a photon density of $5.4 \times I_0$ and a probing field strength of (a) 238 V/cm and (b) 3577 V/cm. (c) Temporal evolution of the differential response between the two probing field strengths.

spectral window from 4.1 to 9.3 meV, where intraexcitonic transitions dominate. Since the Drude background has been effectively removed, this integration yields a direct measure of the exciton oscillator strength at each time delay. Figure 7 shows the normalized exciton oscillator strength as a function of time for various excitation densities. Interestingly, the data cannot be well described by a simple bi-exponential model, similar to our earlier observations. Instead, we apply a tri-exponential fit to extract formation and decay timescales. In stark contrast to the apparent density dependence observed in conventional OPTP data (cf. Fig. 4), the formation dynamics revealed by this differential method are largely independent of excitation density. Across all conditions, we identify three robust timescales: a fast component around ∼10 ps, a slower build up around ∼250 ps, and a density-dependent decay between 1 and 2 ns. These timescales are consistent with those extracted at lower densities with conventional OPTP and provide no evidence for a quasi-instantaneous formation process. Our high-temporal-resolution data thus challenge previous claims of ultrafast or quasi-instantaneous exciton formation. Instead, our results support a continuous, multitimescale formation process that remains largely density independent across the order-of-magnitude variation in excitation density explored here. It is well established that at very low excitation densities, exciton formation proceeds more slowly, consistent with reduced carrier-carrier and carrier-phonon scattering rates [21]. Conversely, as the excitation density approaches the Mott transition, exciton formation is suppressed. These observations indicate the existence of an intermediate density regime—such as the one investigated here—where exciton formation occurs on comparable, largely density-independent timescales.

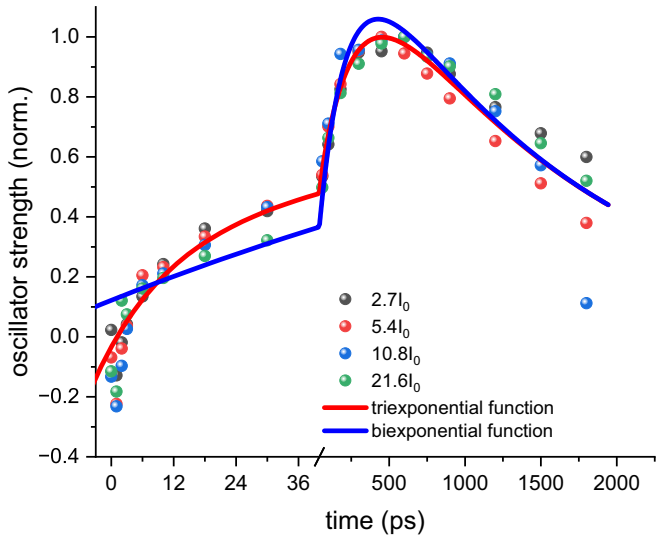

FIG. 7. Normalized oscillator strength for the intraexcitonic transition integrated from 4.1 to 9.3 meV for four excitation densities.

Within this intermediate regime, the slow exciton formation process on timescales around ∼250 ps, as observed in numerous experimental OPTP studies for different semiconductor systems [19–23], can be consistently attributed to the well-established phonon-assisted exciton formation mechanism. In this process, incoherent electron-hole pairs relax into 1*s* excitons through acoustic-phonon scattering, as described in various microscopic and kinetic models [18,30,32,36,42,43]. The resulting formation times of hundreds of picoseconds reflect the weak coupling strength of acoustic phonons and the requirement of energy dissipation for a high conversion of correlations into exciton populations.

The existence of an additional, much faster formation component on ∼10 ps timescales raises questions about its microscopic origin. While interactions with LO phonons have often been invoked as a rapid and efficient exciton formation mechanism [29–32,44], this explanation appears inconsistent with our observations. The fast component shows no dependence on excitation excess energy, and LO-phonon emission is energetically forbidden for excitation close to the band edge, yet rapid exciton formation persists even under these conditions. We therefore attribute the observed ∼10 ps formation dynamics to a geminatelike exciton formation channel [30,45], in which part of the initial Coulomb correlation between electrons and holes is preserved immediately after photoexcitation. Following initial carrier thermalization, a mixed ensemble of uncorrelated carriers and correlated electron-hole pairs coexists. The correlated pairs can evolve into an incoherent exciton population on picosecond timescales through Coulomb-mediated scattering, while the majority of carriers must first build up correlations and subsequently form excitons via the slower phonon-assisted pathway. This picture is consistent with the microscopic theory of exciton formation, in which exciton populations emerge from the decay of coherent interband polarizations through Coulomb and carrier-phonon interactions [18,32,43].

Although pure Coulomb coupling conserves the total energy of the plasma, higher-order Coulomb scattering processes enable energy redistribution among charge carriers. In such events, the binding energy of one correlated pair can be transferred to other electrons or holes, allowing a limited fraction of pairs to relax into Coulomb-bound excitonic states without lattice coupling. Moreover, excitons with large center-of-mass momenta can form even without significant energy loss since their kinetic energy largely compensates the exciton binding energy. These considerations make a correlation-preserving, Coulomb-driven formation channel on a 10 ps timescale physically plausible. Further support for this interpretation comes from the absence of the rapid formation component in indirect-gap semiconductors such as Si [19], Ge [21], and Ge quantum wells [46]. In these materials, strong intervalley phonon scattering transfers charge carriers from the Γ valley to side valleys during or shortly after excitation [47–49]. This intervalley transfer destroys the initial electron-hole Coulomb correlations that would otherwise support the geminatelike channel. As a result, only the slow, phonon-assisted exciton formation on the hundreds-of-picoseconds timescale remains observable.

The key insight provided by our method is that conventional OPTP spectroscopy alone, particularly at higher carrier densities, struggles to reliably distinguish between exciton and plasma contributions. In our case, this always leads to an overestimation of the exciton components, especially at early times. We assume that this overestimation of the exciton fraction with conventional OPTP spectroscopy has led to misinterpretation of the underlying dynamics [20,28]. By eliminating the ambiguity between plasma and exciton responses, our approach provides a consistent and accurate framework for studying exciton formation. It reconciles previously conflicting results in the literature and offers a unified picture of many-body dynamics in GaAs-based quantum well structures across a broad range of excitation conditions.

IV. CONCLUSION

We investigated the THz response of (Ga,In)As/GaAs multiple quantum wells following nonresonant optical excitation. Immediately after excitation, the system exhibits a characteristic Drude-like response from an unbound electron-hole plasma, which gradually evolves into a finite 1*s* exciton population. Exciton formation proceeds on two distinct timescales: a fast component within the first few tens of picoseconds and a slower phase extending over several-hundred picoseconds. Interestingly, while conventional analyses suggest a strong dependence of these timescales on excitation density, our refined methodology reveals that exciton formation dynamics are rather independent of both the excitation density and excess energy within the investigated range. This conclusion is enabled by our different approach that systematically compares THz responses at weak and strong probe field strengths. By exploiting field-induced exciton ionization, we isolate the pure excitonic signal from the overlapping plasma background, even at higher excitation densities where traditional analysis struggles. Our results resolve longstanding ambiguities in the interpretation of time-resolved THz spectroscopy and establish a robust, broadly applicable framework for disentangling exciton and plasma dynamics. This methodology offers clear insight into the intrinsic exciton formation process and is broadly applicable to the study of ultrafast many-body phenomena in semiconductor quantum structures.

ACKNOWLEDGMENTS

Financial support from the Deutsche Forschungsgemeinschaft via the Collaborative Research Center SFB 1083 under Project No. 223848855 is gratefully acknowledged.

DATA AVAILABILITY

The data that support the findings of this article are openly available [46].

[1] C. V. Shank, Investigation of ultrafast phenomena in the femtosecond time domain, Science **233**, 1276 (1986).

[2] A. Othonos, Probing ultrafast carrier and phonon dynamics in semiconductors, J. Appl. Phys. **83**, 1789 (1998).

[3] J. Shah, *Ultrafast Spectroscopy of Semiconductors and Semiconductor Nanostructures* (Springer Science & Business Media, New York, 2013), Vol. 115.

[4] J. Szczytko, L. Kappei, J. Berney, F. Morier-Genoud, M. T. Portella-Oberli, and B. Deveaud, Determination of the exciton formation in quantum wells from time-resolved interband luminescence, Phys. Rev. Lett. **93**, 137401 (2004).

[5] S. W. Koch, M. Kira, G. Khitrova, and H. Gibbs, Semiconductor excitons in new light, Nat. Mater. **5**, 523 (2006).

[6] J. I. Kusano, Y. Segawa, Y. Aoyagi, S. Namba, and H. Okamoto, Extremely slow energy relaxation of a two-dimensional exciton in a GaAs superlattice structure, Phys. Rev. B **40**, 1685 (1989).

[7] T. C. Damen, J. Shah, D. Y. Oberli, D. S. Chemla, J. E. Cunningham, and J. M. Kuo, Dynamics of exciton formation and relaxation in GaAs quantum wells, Phys. Rev. B **42**, 7434 (1990).

[8] R. Eccleston, R. Strobel, W. W. Rühle, J. Kuhl, B. F. Feuerbacher, and K. Ploog, Exciton dynamics in a GaAs quantum well, Phys. Rev. B **44**, 1395 (1991).

[9] P. W. M. Blom, P. J. van Hall, C. Smit, J. P. Cuypers, and J. H. Wolter, Selective exciton formation in thin GaAs/$Al_xGa_{1-x}As$ quantum wells, Phys. Rev. Lett. **71**, 3878 (1993).

[10] D. Robart, X. Marie, B. Baylac, T. Amand, M. Brousseau, G. Bacquet, G. Debart, R. Planel, and J. Gerard, Dynamical equilibrium between excitons and free carriers in quantum wells, Solid State Commun. **95**, 287 (1995).

[11] R. Kumar, A. S. Vengurlekar, S. S. Prabhu, J. Shah, and L. N. Pfeiffer, Picosecond time evolution of free electron-hole pairs into excitons in GaAs quantum wells, Phys. Rev. B **54**, 4891 (1996).

[12] M. Gurioli, P. Borri, M. Colocci, M. Gulia, F. Rossi, E. Molinari, P. E. Selbmann, and P. Lugli, Exciton formation and relaxation in GaAs epilayers, Phys. Rev. B **58**, R13403 (1998).

[13] W. Hoyer, C. Ell, M. Kira, S. W. Koch, S. Chatterjee, S. Mosor, G. Khitrova, H. M. Gibbs, and H. Stolz, Many-body dynamics

and exciton formation studied by time-resolved photoluminescence, Phys. Rev. B **72**, 075324 (2005).

[14] B. Deveaud, B. Sermage, and D. Katzer, Free exciton versus free carrier luminescence in a quantum well, J. Phys. IV **3**, C5-11 (1993).

[15] M. Kira, F. Jahnke, and S. W. Koch, Microscopic theory of excitonic signatures in semiconductor photoluminescence, Phys. Rev. Lett. **81**, 3263 (1998).

[16] S. Chatterjee, C. Ell, S. Mosor, G. Khitrova, H. M. Gibbs, W. Hoyer, M. Kira, S. W. Koch, J. P. Prineas, and H. Stolz, Excitonic photoluminescence in semiconductor quantum wells: Plasma versus excitons, Phys. Rev. Lett. **92**, 067402 (2004).

[17] I. Galbraith, R. Chari, S. Pellegrini, P. J. Phillips, C. J. Dent, A. F. G. van der Meer, D. G. Clarke, A. K. Kar, G. S. Buller, C. R. Pidgeon, B. N. Murdin, J. Allam, and G. Strasser, Excitonic signatures in the photoluminescence and terahertz absorption of a GaAs/Al_xGa_{1-x}As multiple quantum well, Phys. Rev. B **71**, 073302 (2005).

[18] M. Kira, W. Hoyer, T. Stroucken, and S. W. Koch, Exciton formation in semiconductors and the influence of a photonic environment, Phys. Rev. Lett. **87**, 176401 (2001).

[19] T. Suzuki and R. Shimano, Time-resolved formation of excitons and electron-hole droplets in Si studied using terahertz spectroscopy, Phys. Rev. Lett. **103**, 057401 (2009).

[20] R. A. Kaindl, M. A. Carnahan, D. Hägele, R. Lövenich, and D. S. Chemla, Ultrafast terahertz probes of transient conducting and insulating phases in an electron-hole gas, Nature (London) **423**, 734 (2003).

[21] M. Stein, C. Lammers, P. Springer, P.-H. Richter, S. W. Koch, M. Koch, and M. Kira, Density-dependent exciton dynamics and l-valley anisotropy in germanium, Phys. Rev. B **95**, 155207 (2017).

[22] M. Stein, C. Lammers, P.-H. Richter, C. Fuchs, W. Stolz, M. Koch, O. Vänskä, M. J. Weseloh, M. Kira, and S. W. Koch, Dynamics of charge-transfer excitons in type-II semiconductor heterostructures, Phys. Rev. B **97**, 125306 (2018).

[23] R. A. Kaindl, D. Hägele, M. A. Carnahan, and D. S. Chemla, Transient terahertz spectroscopy of excitons and unbound carriers in quasi-two-dimensional electron-hole gases, Phys. Rev. B **79**, 045320 (2009).

[24] R. Groeneveld and D. Grischkowskyt, Picosecond time-resolved far-infrared experiments on carriers and excitons in GaAs–AlGaAs multiple quantum wells, J. Opt. Soc. Am. B **11**, 2502 (1994).

[25] S. Lutgen, T. Albrecht, T. Marschner, W. Stolz, and E. Göbel, Optical properties of symmetrically strained (GaIn) As/Ga (PAs) superlattices grown by metalorganic vapour phase epitaxy, Solid-State Electron. **37**, 905 (1994).

[26] R. Ulbricht, E. Hendry, J. Shan, T. F. Heinz, and M. Bonn, Carrier dynamics in semiconductors studied with time-resolved terahertz spectroscopy, Rev. Mod. Phys. **83**, 543 (2011).

[27] D. Anders, F. Dobener, F. Schäfer, S. Chatterjee, and M. Stein, Inhibited inelastic scattering of incoherent excitons for near-band edge excitations, Phys. Rev. Lett. **132**, 106901 (2024).

[28] P. Steinleitner, P. Merkl, P. Nagler, J. Mornhinweg, C. Schüller, T. Korn, A. Chernikov, and R. Huber, Direct observation of ultrafast exciton formation in a monolayer of WSe_2, Nano Lett. **17**, 1455 (2017).

[29] P. E. Selbmann, M. Gulia, F. Rossi, E. Molinari, and P. Lugli, Coupled free-carrier and exciton relaxation in optically excited semiconductors, Phys. Rev. B **54**, 4660 (1996).

[30] C. Piermarocchi, F. Tassone, V. Savona, A. Quattropani, and P. Schwendimann, Exciton formation rates in GaAs/Al_xGa_{1-x}As quantum wells, Phys. Rev. B **55**, 1333 (1997).

[31] I.-K. Oh, J. Singh, A. Thilagam, and A. S. Vengurlekar, Exciton formation assisted by LO phonons in quantum wells, Phys. Rev. B **62**, 2045 (2000).

[32] K. Siantidis, V. M. Axt, and T. Kuhn, Dynamics of exciton formation for near band-gap excitations, Phys. Rev. B **65**, 035303 (2001).

[33] L. Kappei, J. Szczytko, F. Morier-Genoud, and B. Deveaud, Direct observation of the Mott transition in an optically excited semiconductor quantum well, Phys. Rev. Lett. **94**, 147403 (2005).

[34] B. Deveaud, L. Kappei, J. Berney, F. Morier-Genoud, M. Portella-Oberli, J. Szczytko, and C. Piermarocchi, Excitonic effects in the luminescence of quantum wells, Chem. Phys. **318**, 104 (2005).

[35] A. Hangleiter, Z. Jin, M. Gerhard, D. Kalincev, T. Langer, H. Bremers, U. Rossow, M. Koch, M. Bonn, and D. Turchinovich, Efficient formation of excitons in a dense electron-hole plasma at room temperature, Phys. Rev. B **92**, 241305(R) (2015).

[36] W. Hoyer, M. Kira, and S. W. Koch, Influence of Coulomb and phonon interaction on the exciton formation dynamics in semiconductor heterostructures, Phys. Rev. B **67**, 155113 (2003).

[37] R. Huber, R. A. Kaindl, B. A. Schmid, and D. S. Chemla, Broadband terahertz study of excitonic resonances in the high-density regime in GaAs/Al_xGa_{1-x}As quantum wells, Phys. Rev. B **72**, 161314(R) (2005).

[38] M. Stein, F. Schäfer, and L. Gomell, Inelastic electron-exciton scattering in bulk germanium, Phys. Rev. B **99**, 144310 (2019).

[39] B. Ewers, N. S. Köster, R. Woscholski, M. Koch, S. Chatterjee, G. Khitrova, H. M. Gibbs, A. C. Klettke, M. Kira, and S. W. Koch, Ionization of coherent excitons by strong terahertz fields, Phys. Rev. B **85**, 075307 (2012).

[40] F. Sekiguchi, T. Mochizuki, C. Kim, H. Akiyama, L. N. Pfeiffer, K. W. West, and R. Shimano, Anomalous metal phase emergent on the verge of an exciton Mott transition, Phys. Rev. Lett. **118**, 067401 (2017).

[41] M. Stein, C. Lammers, J. Steiner, P. Richter, S. Koch, M. Koch, and M. Kira, Exciton ionization by THz pulses in germanium, J. Phys. B: At. Mol. Opt. Phys. **51**, 154001 (2018).

[42] M. Gulia, F. Rossi, E. Molinari, P. E. Selbmann, and P. Lugli, Phonon-assisted exciton formation and relaxation in GaAs/Al_xGa_{1-x}As quantum wells, Phys. Rev. B **55**, R16049 (1997).

[43] M. Kira and S. W. Koch, Many-body correlations and excitonic effects in semiconductor spectroscopy, Prog. Quantum Electron. **30**, 155 (2006).

[44] M. Umlauff, J. Hoffmann, H. Kalt, W. Langbein, J. M. Hvam, M. Scholl, J. Söllner, M. Heuken, B. Jobst, and D. Hommel, Direct observation of free-exciton thermalization in quantum-well structures, Phys. Rev. B **57**, 1390 (1998).

[45] K. Mourzidis, V. Jindal, M. Glazov, A. Balocchi, C. Robert, D. Lagarde, P. Renucci, L. Lombez, T. Taniguchi, K. Watanabe *et al.*, Exciton formation in two-dimensional semiconductors, Phys. Rev. X **15**, 031078 (2025).

[46] D. Anders, Data for "exciton formation dynamics in (Ga,In,)As quantum wells" (2025), https://doi.org/10.22029/jlupub-20089.2.

[47] S. A. Claussen, E. Tasyurek, J. E. Roth, and D. A. Miller, Measurement and modeling of ultrafast carrier dynamics and transport in germanium/silicon-germanium quantum wells, Opt. Express **18**, 25596 (2010).

[48] C. Lange, N. S. Köster, S. Chatterjee, H. Sigg, D. Chrastina, G. Isella, H. von Känel, B. Kunert, and W. Stolz, Comparison of ultrafast carrier thermalization in $Ga_xIn_{1-x}As$ and Ge quantum wells, Phys. Rev. B **81**, 045320 (2010).

[49] E. J. Loren, J. Rioux, C. Lange, J. E. Sipe, H. M. van Driel, and A. L. Smirl, Hole spin relaxation and intervalley electron scattering in germanium, Phys. Rev. B **84**, 214307 (2011).